Phase transitions and phase separations in an $S=1$ pseudospin-electron model: Application of the model to the intercalated crystals

I. V. Stasyuk and Yu. I. Dublenych
Institute for Condensed Matter Physics of the National Academy of Sciences of Ukraine, 1 Svientsitskii Street, 79011 Lviv, Ukraine
(Received 18 March 2005; revised manuscript received 8 November 2005; published 30 December 2005)

A pseudospin-electron model based on the Blume-Emery-Griffiths model is used to describe the phase transitions and phase separations in intercalated crystals. It is shown that, due to the one-site character of the electron-electron and pseudospin-electron interactions, the partition function of such a model can be presented as the product of the partition functions of independent pseudospin (with two shifted parameters) and electron subsystems. The phase diagrams of the model as well as the phase separation diagrams and the dependencies of the concentration of intercalated particles on their chemical potential are constructed: *exactly* for zero temperature and in the mean field approximation for nonzero one. It is shown that in certain interval of chemical potential values the direct interaction between intercalated particles and basic layer electrons leads to the separation into phases with different particle and electron concentrations.

DOI: 10.1103/PhysRevB.72.224209 PACS number(s): 71.10.Fd, 71.20.Tx, 75.10.Hk, 05.50.+q

I. INTRODUCTION

During the last decades the studies of intercalation processes in layered crystals have been progressing very intensively. The reason is the plenty of possibilities of their practical use: in hydrogen storage systems,[1] rechargeable high-energy batteries,[2,3] electrochromic devices,[4] superconductors,[5] etc.

The intercalation is usually considered as an absorption of guest particles on a host lattice. The hosts can be, for instance, transition metal dichalcogenides, lead and bismuth iodides, oxides of transition metals and graphite, mica, as well as less studied A^3B^6 and $A_2^5B_3^6$ type compounds (InSe, GaSe, Bi_2Te_3, Bi_2Se_3). Due to the weak van der Waals bonding between the layers of these crystals, the guest particles can be easily inserted. These latter can be different ions, atoms, or molecules: lithium and halogen ions, hydrogen, fluorine, and water molecules, organic molecules [for instance, aniline $C_6H_5NH_2$ and piperidine $CH_2(CH_2)_4H$ in mica], OH^- ions, etc.

Guest particles occupy some energetically favorable positions in the van der Waals gap between basic layers of the crystal and form a two-dimensional lattice. Therefore, traditionally lattice gas models have been used for description of the intercalated particle subsystem in layered crystals.[2] If all positions are equivalent and intercalated particles have no dipole moment, one can use the spin-$\frac{1}{2}$ Ising model. The negative value of spin corresponds to the situation when there is no particle at a lattice site, the positive one corresponds to the reverse situation or vice versa. However, this simple model does not suit the case of the intercalation of *dipole* particles. If dipole moment of guest particles is perpendicular to basic layers of the crystal (both senses being of the same probability at zero external field), then three states for each site are possible and, for describing the dipole lattice gas of intercalated particles, we can use the spin-1 Ising model [the Blume-Emery-Griffiths (BEG) model]. This model is also applicable in the case when particles have no dipole moment but can occupy two different positions: the one nearer to the lower neighboring basic layer or the one nearer to the upper one, the situation is equivalent to the presence of dipole moment. This is observed, for instance, in some transition metal dichalcogenides, where intercalated atoms occupy asymmetric tetrahedral sites,[6] and in well-known TiS_2 intercalated by alkali metal atoms (Li or Na), where these atoms occupy trigonal sites (if their concentration is not too large).[7] Another example of using a spin-1 Ising model to intercalation compounds is given in Ref. 8. There a special spin-1 Ising model on the triangular lattice with nonzero interactions up to third nearest neighbors is applied to *ternary* graphite intercalation compounds.

However, pure pseudospin models have an essential disadvantage: they do not take explicitly into account the direct interaction between the intercalated particles and the atoms of basic layers. To describe the intercalation process, we use a pseudospin-electron model based on the BEG one. This model takes into account the above-mentioned interaction explicitly though in a simplified way: as an one-site interaction of pseudospins with the electron subsystem. There is no electron transfer but the direct pseudospin-pseudospin interaction is considered. One can find a brief review of the pseudospin-electron model and related bibliography in Ref. 9. The model similar to the considered one but with pseudospin $S=\frac{1}{2}$ has been studied in Ref. 10.

Thus, the model that we consider combines two subsystems: pseudospin and electron ones. It will be shown that, due to the fact that both the electron-electron and pseudospin-electron interactions are of the one-site type, the partition function of such a model splits into a product of those for electron and pseudospin subsystems. The external field and the single-ion anisotropy of the pseudospin subsystem will be shifted and will depend on the temperature and the parameters related to the electrons. Hence, the influence of the electron subsystem can be taken into account exactly and the study of phase transitions and phase separations in this model can be reduced to the study of these phenomena in the BEG model.

A very important problem is the choice of the signs of the bilinear and biquadratic (dipole-dipole and quadruple-

quadruple, respectively) interactions in the model. The direct electrostatic interaction of charged particles or dipoles with the same orientation perpendicularly to the plane, where they reside, has the positive sign (repulsion). But there is also an indirect interaction between guest particles in intercalated crystals, via the electron subsystem of covalently bonded atoms of basic layers. This indirect interaction, depending on band structure and occupation of electron states, can be negative (attraction).[11] Moreover, the effective interaction between guest particles significantly depends on local deformations of the crystal lattice, caused by the presence of intercalated particles.[12] We will consider the case where the bilinear interaction is negative and the biquadratic interaction is less than the bilinear one taken with the opposite sign. In this case the translational symmetry of the lattice does not change, i.e., the lattice does not split into two or more sublattices.

Our paper is organized as follows: in Sec. II we introduce a simplified pseudospin-electron model on the base of the BEG one and we reduce it to a pure pseudospin model; in Sec. III we investigate phase transitions and phase separations in the model at zero temperature. In Sec. IV the symmetry of the most general spin-1 Ising Hamiltonian is studied. All results of Secs. II, III, and IV are exact. In Sec. V we analyze phase transitions and phase separations in the BEG model within the mean field approximation. In Secs. IV and V we reviewed some already known results but also present several new ones. In Sec. VI we show the influence of electrons on phase coexistence and phase separation surfaces and present the dependencies of average number of guest particles per site on their chemical potential. In Sec. VII we draw some conclusions.

II. HAMILTONIAN, PARTITION FUNCTION, AND FORMULA FOR THE AVERAGE ELECTRON NUMBER PER SITE

Consider a layered crystal with dipole particles intercalated between its layers and directed perpendicularly to them. Each intercalated particle interacts with other particles and with one or two electrons at the neighboring site of the basic layer. There is also the one-site interaction between electrons. We will describe the crystal by a lattice model. The state of the ith lattice site is characterized by two numbers: $|S_i^z, n_{ei}\rangle$. $S_i^z = 0, -1, +1$ when the dipole particle on the ith site is absent, orientated down or up, respectively; n_{ei} is the number of electrons at the ith site (0, 1, or 2). $S_i^{z^2}$ is then the number of dipole particles on the ith site (0 or 1).

We can write the Hamiltonian of such a model using the pseudospin formalism

$$H = H_s + H_{se} + H_e. \tag{1}$$

Here

$$H_s = -\frac{1}{2}\sum_{ij} J_{ij} S_i^z S_j^z - \frac{1}{2}\sum_{ij} K_{ij} S_i^{z^2} S_j^{z^2} + \sum_i \left(-hS_i^z + E_0 S_i^{z^2}\right) \tag{2}$$

is the Hamiltonian of the pseudospin $S=1$ model (the BEG model). The bilinear and biquadratic terms describe the interactions between pseudospins that are dependent and independent on the orientation, respectively, i.e., the dipole-dipole and charge-charge (or particle-particle) interactions between intercalated particles. $-hS_i^z$ is the energy of the ith pseudospin in the external field and E_0 is the single-ion anisotropy. $-E_0$ is the chemical potential of intercalated particles.

The electron subsystem is described by the Hamiltonian H_e

$$H_e = \frac{U}{2}\sum_i n_{ei}(n_{ei} - 1) - \mu \sum_i n_{ei}, \tag{3}$$

where U is the Hubbard electron correlation at a site, and μ is the chemical potential of electrons. The Hamiltonian H_{se} links together the pseudospin and electron subsystems

$$H_{se} = g\sum_i n_{ei} S_i^z + \rho \sum_i n_{ei} S_i^{z^2}, \tag{4}$$

where g and ρ are the energies of the pseudospin-electron interaction dependent and independent on the pseudospin orientation, respectively. Hamiltonian (1) can be represented as a sum of two-site and one-site Hamiltonians

$$H = \sum_{ij} H_{ij} + \sum_i H_i. \tag{5}$$

For the study of the phase transitions and phase separations in the system let us evaluate its partition function. Consider states where pseudospins on k sites are orientated up, at m sites down, and at the rest $N-k-m (k+m \leqslant N)$ sites pseudospins are equal to zero. It is easy to see that the contribution of these states in the partition function is as follows:

$$\begin{aligned} Z_{km} &= \left(\sum_{\langle km\rangle} e^{-\beta\sum_{ij} H_{ij}}\right) e^{-\beta[-h(k-m)+E_0(k+m)]}\left(1 + e^{-\beta(2g+2\rho+U-2\mu)}\right. \\ &\quad \left. + 2e^{-\beta(g+\rho-\mu)}\right)^k \left(1 + e^{-\beta(-2g+2\rho+U-2\mu)} + 2e^{-\beta(-g+\rho-\mu)}\right)^m \\ &\quad \times \left(1 + e^{-\beta(U-2\mu)} + 2e^{\beta\mu}\right)^{N-k-m} \\ &= \left(\sum_{\langle km\rangle} e^{-\beta\Sigma_{ij} H_{ij}}\right) \exp\left[\beta\left(-E_0 + \frac{1}{2\beta}\ln\frac{r}{t} + \frac{1}{\beta}\ln\frac{t}{s}\right)\right. \\ &\quad \left. \times (k+m)\right] \exp\left[\beta\left(h + \frac{1}{2\beta}\ln\frac{r}{t}\right)(k-m)\right] s^N, \end{aligned} \tag{6}$$

where

$$\begin{aligned} r &= 1 + e^{-\beta(2g+2\rho+U-2\mu)} + 2e^{-\beta(g+\rho-\mu)}, \\ t &= 1 + e^{-\beta(-2g+2\rho+U-2\mu)} + 2e^{-\beta(-g+\rho-\mu)}, \\ s &= 1 + e^{-\beta(U-2\mu)} + 2e^{\beta\mu}, \end{aligned} \tag{7}$$

$\langle km\rangle$ means that the sum is over the states with k pseudospins orientated up and m down. The total partition function is equal to

$$Z = \sum_{km} Z_{km}. \tag{8}$$

Expression (6) without the factor s^N represents the partition function of the pseudospin model described by the Hamil-

tonian H_s, but with the energies $\tilde{h}$ and $\tilde{E}_0$ (instead of h and E_0) that depend on the electron parameters of the Hamiltonian H and on the temperature

$$\tilde{h} = h + \frac{1}{2\beta}\ln\frac{r}{t} = h + \frac{1}{2\beta}\ln\frac{r}{s} - \frac{1}{2\beta}\ln\frac{t}{s},$$

$$\tilde{E}_0 = E_0 - \frac{1}{2\beta}\ln\frac{r}{t} - \frac{1}{\beta}\ln\frac{t}{s}$$

$$= E_0 - \frac{1}{2\beta}\ln\frac{r}{s} - \frac{1}{2\beta}\ln\frac{t}{s}. \quad (9)$$

Let us consider the thermodynamic potential of the system per site

$$\omega = -\frac{1}{\beta N}\ln Z = -\frac{1}{\beta}\ln s - \frac{1}{\beta N}\ln\sum_{km}\left(\sum_{\langle km\rangle} e^{-\beta\Sigma_{ij}H_{ij}}\right) \times e^{-\beta\tilde{E}_0(k+m)} e^{\beta\tilde{h}(k-m)}. \quad (10)$$

The average number of particles, the average number of electrons, and the average dipole moment per site are expressed in terms of derivatives of ω

$$n = \langle S_i^{z^2}\rangle = \frac{\partial\omega}{\partial E_0} = \frac{\partial\omega}{\partial\tilde{E}_0}, \quad n_e = -\frac{\partial\omega}{\partial\mu},$$

$$\eta = \langle S_i^z\rangle = -\frac{\partial\omega}{\partial h} = -\frac{\partial\omega}{\partial\tilde{h}}. \quad (11)$$

The expression for the average number of electrons per site can be written as follows:

$$n_e = -\frac{\partial\omega}{\partial\mu} = -\frac{\partial\omega}{\partial\tilde{E}_0}\frac{\partial\tilde{E}_0}{\partial\mu} - \frac{\partial\omega}{\partial\tilde{h}}\frac{\partial\tilde{h}}{\partial\mu} + \frac{1}{\beta}\frac{\partial\ln s}{\partial\mu}$$

$$= -n\frac{\partial\tilde{E}_0}{\partial\mu} + \eta\frac{\partial\tilde{h}}{\partial\mu} + \frac{1}{\beta s}\frac{\partial s}{\partial\mu}$$

$$= \frac{1}{2\beta r}\frac{\partial r}{\partial\mu}(n+\eta) + \frac{1}{2\beta t}\frac{\partial t}{\partial\mu}(n-\eta) + \frac{1}{\beta s}\frac{\partial s}{\partial\mu}(1-n). \quad (12)$$

Taking into account expressions (7) for r,t,s, after simple transformations we will get

$$n_e = 2 - c_1(n+\eta) - c_2(n-\eta) - 2c_3(1-n), \quad (13)$$

where the following notations were introduced:

$$c_1 = \frac{1+e^{-\beta(g+\rho-\mu)}}{1+e^{-\beta(2g+2\rho+U-2\mu)}+2e^{-\beta(g+\rho-\mu)}},$$

$$c_2 = \frac{1+e^{-\beta(-g+\rho-\mu)}}{1+e^{-\beta(-2g+2\rho+U-2\mu)}+2e^{-\beta(-g+\rho-\mu)}},$$

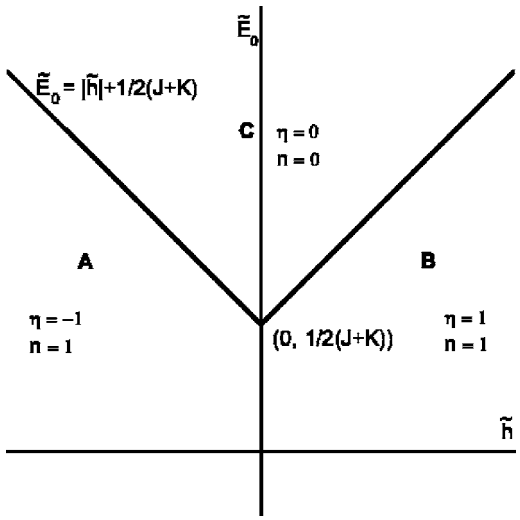

FIG. 1. Phase diagram of the BEG model in the $(\tilde{h},\tilde{E}_0)$ plane at zero temperature. Three different phases (A, B, C) are indicated.

$$c_3 = \frac{1+e^{\beta\mu}}{1+e^{-\beta(U-2\mu)}+2e^{\beta\mu}}. \quad (14)$$

Note, that $n_e \to 0$ if $\mu \to -\infty$, and $n_e \to 2$ if $\mu \to +\infty$. Relation (13) expresses the electron chemical potential in terms of the concentrations of electrons and intercalated particles and the average dipole moment of particles.

III. PHASE TRANSITIONS AND PHASE SEPARATIONS AT ZERO TEMPERATURE

In the previous section we have reduced the partition function of our pseudospin-electron model to the partition function of the pure pseudospin model. Now we have to consider the pseudospin model described by the Hamiltonian (2) (but with the parameters $\tilde{h}$ and $\tilde{E}_0$ instead of h and E_0). For the first time this model was used by Blume, Emery, and Griffiths in the context of superfluidity and phase separation in ^{3}He-^{4}He mixtures.[13] Therefore it is also called the Blume-Emery-Griffiths model. It was investigated in many studies, particularly in Refs. 13–18 in the mean field approximation. Later we will use this approximation as well.

Let us consider the Hamiltinian

$$H_s = -J\sum_{\langle ij\rangle} S_i^z S_j^z - K\sum_{\langle ij\rangle} S_i^{z^2} S_j^{z^2} + \sum_i (-\tilde{h}S_i^z + \tilde{E}_0 S_i^{z^2}), \quad (15)$$

where $\langle ij\rangle$ means that the sum is over nearest-neighbor pairs only, J and K are the strengths of the bilinear and biquadratic interactions, respectively.

First of all, we will consider the model at zero temperature, i.e., the ground states of the system. In Ref. 19 the exact ground-state diagrams for the most general spin-1 Ising model on different lattices were constructed. We will use the results of this study. It is shown there that in the case of nearest neighbor interaction only the lattice does not split into two sublattices if $J \geqslant 0$ and $J+K \geqslant 0$.

The ground-state diagram for this case is shown in Fig. 1.

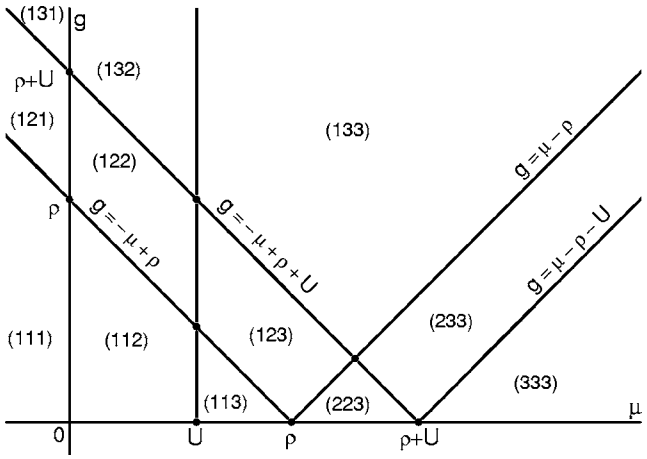

FIG. 2. Regions of different behavior of the shifts Δh and ΔE_0 at zero temperature. $0 \leqslant U < \rho$. The notations of regions are explained in the text.

Three phases are possible: A, B, and C. When moving from the phase A to the phase B the sign of η changes and n remains the same; when moving from the phase A or B to the phase C both values change discontinuously. If $J \neq 0$, the similar behavior is observed at nonzero temperature.

Now let us consider the shifts of the phase diagram caused by electrons. To do this we shall investigate the zero temperature behavior of the values $(1/\beta)\ln r$, $(1/\beta)\ln t$, and $(1/\beta)\ln s$, in terms of which the shifts are expressed

$$\Delta h = \frac{1}{2}\left(\frac{1}{\beta}\ln r - \frac{1}{\beta}\ln t\right),$$

$$\Delta E_0 = -\frac{1}{2}\left(\frac{1}{\beta}\ln r + \frac{1}{\beta}\ln t\right) + \frac{1}{\beta}\ln s. \tag{16}$$

$$q_1 = \lim_{T\to 0}\frac{1}{\beta}\ln r = \begin{cases} 0, & -g-\rho+\mu \leqslant 0 \quad (1) \\ -g-\rho+\mu, & 0 < -g-\rho+\mu \leqslant U \quad (2) \\ 2(-g-\rho+\mu)-U, & -g-\rho+\mu > U \quad (3), \end{cases}$$

$$q_2 = \lim_{T\to 0}\frac{1}{\beta}\ln t = \begin{cases} 0, & g-\rho+\mu \leqslant 0 \quad (1) \\ g-\rho+\mu, & 0 < g-\rho+\mu \leqslant U \quad (2) \\ 2(g-\rho+\mu)-U, & g-\rho+\mu > U \quad (3), \end{cases}$$

$$q_3 = \lim_{T\to 0}\frac{1}{\beta}\ln s = \begin{cases} 0, & \mu \leqslant 0 \quad (1) \\ \mu, & 0 < \mu \leqslant U \quad (2) \\ 2\mu - U, & \mu > U \quad (3). \end{cases} \tag{17}$$

The regions of different behavior of the shifts Δh and ΔE_0 are shown in Fig. 2 in the (μ, g) plane when $0 \leqslant U < \rho$. We employed the following notations for the regions: the first number in the parentheses denotes which of inequalities, (1), (2), or (3), holds for q_1 in Eq. (17), the second and the third numbers correspond to q_2 and q_3, respectively. The coefficients c_1, c_2, c_3 [see Eq. (14)] tend to 1 in case (1), to $\frac{1}{2}$ in case (2), and to 0 in case (3).

TABLE I. The shifts Δh and ΔE_0 and the jumps of n_e for different regions at zero temperature.

Region	Δh	ΔE_0	n_e
(111)	0	0	$0 \to 0 \leftarrow 0$
(112)	0	μ	$0 \to 1 \leftarrow 0$
(113)	0	$2\mu - U$	$0 \to 2 \leftarrow 0$
(121)	$(-g+\rho-\mu)/2$	$(-g+\rho-\mu)/2$	$1 \to 0 \leftarrow 0$
(122)	$(-g+\rho-\mu)/2$	$(-g+\rho+\mu)/2$	$1 \to 1 \leftarrow 0$
(123)	$(-g+\rho-\mu)/2$	$(-g+\rho+3\mu)/2-U$	$1 \to 2 \leftarrow 0$
(131)	$-g+\rho-\mu+U/2$	$-g+\rho-\mu+U/2$	$2 \to 0 \leftarrow 0$
(132)	$-g+\rho-\mu+U/2$	$-g+\rho+U/2$	$2 \to 1 \leftarrow 0$
(133)	$-g+\rho-\mu+U/2$	$-g+\rho+\mu-U/2$	$2 \to 2 \leftarrow 0$
(222)	$-g$	ρ	$1 \to 1 \leftarrow 1$
(223)	$-g$	$\rho+\mu-U$	$1 \to 2 \leftarrow 1$
(232)	$(-3g+\rho-\mu+U)/2$	$(-g+3\rho-\mu+U)/2$	$2 \to 1 \leftarrow 1$
(233)	$(-3g+\rho-\mu+U)/2$	$(-g+3\rho+\mu-U)/2$	$2 \to 2 \leftarrow 1$
(333)	$-2g$	2ρ	$2 \to 2 \leftarrow 2$

In Table I the shifts Δh and ΔE_0 are given for each region and the changes of the average electron number per site n_e at the phase transitions when the field h is fixed are indicated. The right arrow corresponds to the transition at $\tilde{h} < 0$ ($h < -\Delta h$, η jumps from -1 to 0), and the left arrow corresponds to the transition at $\tilde{h} > 0$ ($h > -\Delta h$, η jumps from $+1$ to 0). In both cases the average number n of intercalated particles per site jumps from 1 to 0. The phase coexistence line is determined by the equation

$$E_0 + \Delta E_0 = |h + \Delta h| + \frac{J+K}{2}. \tag{18}$$

Up to now we have considered the grand canonical ensemble where neither the number of intercalated particles nor the number of electrons were fixed. Let us consider now the case when the number of electrons is fixed. If, at nonzero temperature, one constructed the graphs of $n_e(-E_0)$ dependency at different values of the electron chemical potential μ (all other parameters and the temperature are being fixed), one could see that if the temperature does not exceed a certain value, then in the $(-E_0, n_e)$ plane there is the region, the points of which do not satisfy the condition of absolute thermodynamic stability at any μ. If the parameters E_0 and n_e are such that the point $(-E_0, n_e)$ drops into this region, then the separation into two phases with different electron and particle concentrations occurs in the system. The separation regions can be also considered in the (θ, n_e) or (h, n_e) plane (θ denotes the thermodynamic temperature), i.e., the separation region is four-dimensional [in the $(n_e, -E_0, h, \theta)$ space]. As the temperature increases it becomes narrower and completely disappears at the critical temperature. The separation regions can be also considered in the (n, μ, h, θ) space.

TABLE II. Conditions when the separation into phases with $n_e=0$ and $n_e=2$ exists at zero temperature.

U		g		h
0	ρ	0	$\rho-U$	Arbitrary
		$\rho-U$	ρ	$h>(g-\rho+U)/2$
		ρ	$\rho+U$	$h>g-\rho+U/2$
ρ	2ρ	0	$U-\rho$	Absent
		$U-\rho$	ρ	$h>(g-\rho+U)/2$
		ρ	$\rho+U$	$h>g-\rho+U/2$
2ρ	∞	0	$U-\rho$	Absent
		$U-\rho$	$\rho+U$	$h>g-\rho+U/2$
0	∞	$\rho+U$	∞	$h<g-\rho-U/2$
				$h>g-\rho+U/2$

Let us construct the phase separation regions in the $(n_e, -E_0)$ plane at zero temperature. The results obtained above should be supplemented by an additional suggestion that the phase coexistence line at $h=0$ and nonzero temperature exists if $J\neq 0$ and does not exist if $J=0$, and two other lines exist in both cases. This suggestion is based on the results within the mean field approximation given below.

If the interaction g is such that when changing μ from $-\infty$ to $+\infty$ one crosses regions (113) $(0<U<\rho)$, (131) $(g>\rho+U)$, (123), or (133), then the region of separation into the phases with $n_e=0$ and $n_e=2$ can exist. Region (113) always produces such a separation, regardless of the value of h. The conditions that shall be satisfied for the separation into phases with $n_e=0$ and $n_e=2$ exists are given in Table II.

If a region of separation into the phases with $n_e=0$ and $n_e=2$ exists in the (E_0, n_e) plane at zero temperature, then the total separation region occurs between the following values of E_0:

$$E_{00}=|h|+\frac{J+K}{2} \quad \text{and} \quad E_{02}=|h-2g|-2\rho+\frac{J+K}{2}. \tag{19}$$

These values correspond to the regions (111) and (333), respectively. If there is no separation into the phases with $n_e=0$ and $n_e=2$, then between E_{00} and E_{01} there is a separation into the phases with $n_e=0$ and $n_e=1$, and between E_{01} and E_{02} into the phases with $n_e=1$ and $n_e=2$. The value E_{01} is as follows:

$$E_{01}=|h-g|-\rho+\frac{J+K}{2}, \tag{20}$$

if $\mu=h-g+\rho+U/2$ lays beyond region (132), or

$$E_{01}=g-\rho-\frac{U}{2}+\frac{J+K}{2}, \tag{21}$$

if $\mu=h-g+\rho+U/2$ drops into region (132). Thus, changing the field h, one can control the width of the separation region.

Different types of separation regions at zero temperature and $J=0$ are shown in Fig. 3. If $J\neq 0$ then the phase transitions at $\tilde{h}=0$ exist also at nonzero temperature and the separation pattern can be more complicated (see Fig. 8). The reason is that at $h\neq 0$ such $\mu=\mu_0$ can exist that $h+\Delta h=0$, and the phase transition from $\tilde{h}<0$ to $\tilde{h}>0$ occurs at this μ_0. Then n_e changes discontinuously and that leads to the appearance of the separation region that corresponds to the phase coexistence line $\tilde{h}=0$ and extends up to the infinite value of $-E_0$. As one can see the shape of the separation region at $T=0$ does not depend on the bilinear and biquadratic couplings.

IV. SYMMETRY OF THE BEG HAMILTONIAN

Consider now the BEG model at arbitrary temperature. To complete the exact results in this model let us consider, as it is done in Ref. 13, the symmetry transformations of the most general spin-1 Ising Hamiltonian

$$H_I=-J\sum_{\langle ij\rangle}S_i^zS_j^z-K\sum_{\langle ij\rangle}S_i^{z^2}S_j^{z^2}-C\sum_{\langle ij\rangle}(S_i^{z^2}S_j^z+S_i^zS_j^{z^2})+\sum_{\langle ij\rangle}(-\tilde{h}S_i^z+\tilde{E}_0S_i^{z^2}). \tag{22}$$

If $C=0$ it becomes the BEG Hamiltonian.

There are three transformations which transform pseudospins 1 in -1, 0 in 1, 0 in -1 and vice versa, leaving, respectively, pseudospins with values 0, -1, and 1 intact. These are

$$S_i^z\rightarrow -S_i^z, \tag{23}$$

$$S_i^z\rightarrow 1+\tfrac{1}{2}S_i^z-\tfrac{3}{2}S_i^{z^2}, \tag{24}$$

$$S_i^z\rightarrow -1+\tfrac{1}{2}S_i^z+\tfrac{3}{2}S_i^{z^2}. \tag{25}$$

Other possible transformations are the linear combinations of these ones. The transformed parameters of Hamiltonian (15) are as follows:

$$J_1=J,\quad K_1=K,\quad C_1=-C,\quad \tilde{h}_1=-\tilde{h},\quad \tilde{E}_{01}=\tilde{E}_0, \tag{26}$$

for transformation (23),

$$J_2=\tfrac{1}{4}(J+K-2C),$$

$$K_2=\tfrac{1}{4}(9J+K+6C),$$

$$C_2=\tfrac{1}{4}(-3J+K+2C),$$

$$\tilde{h}_2=\tfrac{1}{2}(J-K+\tilde{h}+\tilde{E}_0),$$

$$\tilde{E}_{02}=\tfrac{1}{2}(3J+K+4C+3\tilde{h}-\tilde{E}_0), \tag{27}$$

for transformation (24), and

$$J_3=\tfrac{1}{4}(J+K+2C),$$

$$K_3=\tfrac{1}{4}(9J+K-6C),$$

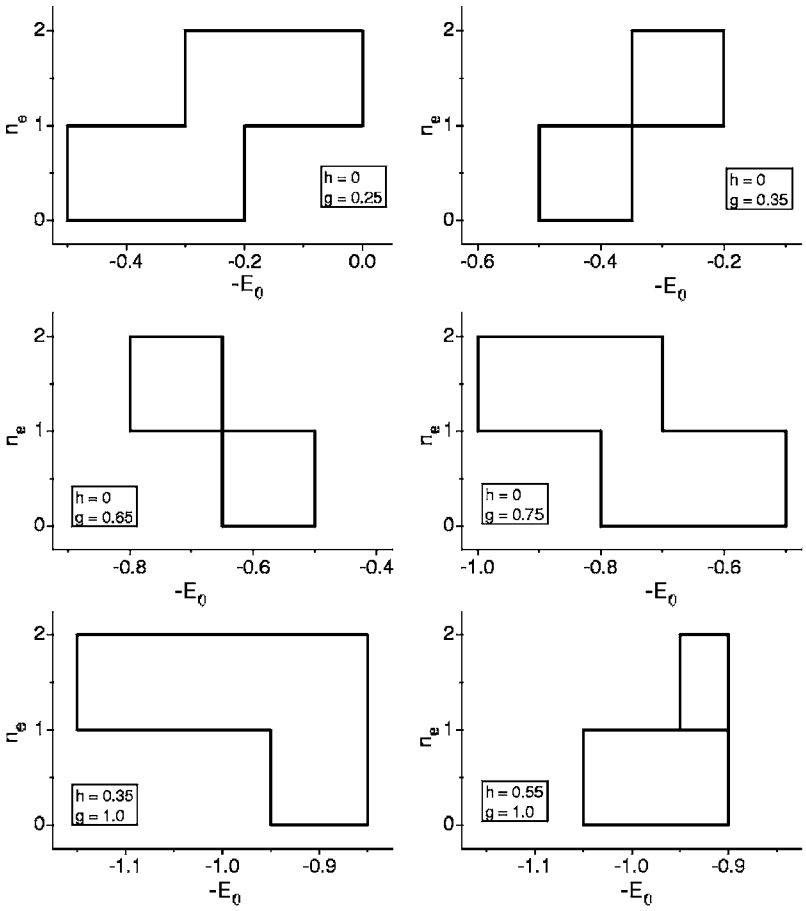

FIG. 3. Phase separation at zero temperature in $(-E_0, n_e)$ plane. $J=0$, $K=0.25$, $\rho=0.5$, $U=0.2$. If n_e and E_0 are such that the point $(-E_0, n_e)$ drops into the separation region, the separation into two phases with different values of n_e (0, 1, or 2) and n (0 and 1) occurs at the same value of E_0.

$$C_3 = \tfrac{1}{4}(3J - K + 2C),$$

$$\tilde{h}_3 = \tfrac{1}{2}(-J + K + \tilde{h} - \tilde{E}_0),$$

$$\tilde{E}_{03} = \tfrac{1}{2}(3J + K - 4C - 3\tilde{h} - \tilde{E}_0), \tag{28}$$

for transformation (25). Equalities (26) yield the symmetry of the phase diagram with respect to the $\tilde{h}=0$ plane. If $K=3J$ and $C=0$, then only two parameters, $\tilde{h}$ and $\tilde{E}_0$, change in Eqs. (27) and (28), the rest do not change. Hence, in this case the transformations

$$\tilde{h} \to -J + \tfrac{1}{2}(\tilde{h} + \tilde{E}_0),$$

$$\tilde{E}_0 \to K + \tfrac{1}{2}(3\tilde{h} - \tilde{E}_0) \tag{29}$$

and

$$\tilde{h} \to J + \tfrac{1}{2}(\tilde{h} - \tilde{E}_0),$$

$$\tilde{E}_0 \to K + \tfrac{1}{2}(-3\tilde{h} - \tilde{E}_0) \tag{30}$$

map the phase diagram in the $(\tilde{h}, \tilde{E}_0, \theta)$ space into itself. This fact will be used in the following section, when we will have to deal with an analog of the van Laar point.[20]

V. PHASE TRANSITIONS IN THE BEG MODEL: MEAN FIELD APPROXIMATION

All results that we obtained above are exact. To study the phase transitions and the phase separations in the BEG model (2) (with $\tilde{h}$ and $\tilde{E}_0$ instead of h and E_0) at arbitrary temperature let us use the mean field approximation. Here, we will mainly review some results from Refs. 13–18, however, some new results will be presented as well: the very important equation for the critical lines, the equation for the coexistence point of four phases, the equation for the van Laar point in the mean field approximation.

A. Self-consistent equations

The Hamiltonian of the BEG model in the mean field approximation reads as follows:

$$H_{MF} = NJ\eta^2 + \frac{N}{2}Kn^2 + \sum_i [-(\tilde{h} + J\eta)S_i^z + (\tilde{E}_0 - Kn)S_i^{z^2}]. \tag{31}$$

Here and thereafter we will use the notations

$$J = \sum_j J_{ij}, \quad K = \sum_j K_{ij}. \tag{32}$$

The thermodynamic potential per site is given by

$$\omega = \frac{J}{2}\eta^2 + \frac{K}{2}n^2 - \frac{1}{\beta}\ln(1 + e^{-\beta(-\tilde{h}-J\eta+\tilde{E}_0-Kn)} + e^{-\beta(\tilde{h}+J\eta+\tilde{E}_0-Kn)}). \tag{33}$$

The self-consistent equations read as follows:

$$e^{2\beta(\tilde{h}+J\eta)} = \frac{n+\eta}{n-\eta},$$

$$e^{2\beta(\tilde{E}_0-Kn)} = \frac{4(1-n)^2}{n^2-\eta^2}. \tag{34}$$

Taking into account Eqs. (34), one can rewrite the expression for the thermodynamic potential as follows:

$$\omega = \frac{J}{2}\eta^2 + \frac{K}{2}n^2 + \frac{1}{\beta}\ln(1-n). \tag{35}$$

Equations (34) yields the relation between n and η

$$n = \eta\ \mathrm{cth}[\beta(\tilde{h}+J\eta)] \tag{36}$$

or

$$\eta^2 = n^2 - 4(1-n)^2 e^{-2\beta(\tilde{E}_0-Kn)}. \tag{37}$$

Let us study the phase transition pattern given by Eqs. (34) and (35). The phase diagram in the $(\tilde{h},\tilde{E}_0)$ plane at zero temperature will be the same as in Fig. 1: the mean field approximation leads to the exact result at zero temperature.

B. Critical lines

Now we will write the equations for the critical lines. They can be found from the condition that both the derivatives $d\tilde{h}/d\eta$ and $d^2\tilde{h}/d\eta^2$ are equal to zero. Differentiating twice Eqs. (34), setting $d\tilde{h}/d\eta$ and $d^2\tilde{h}/d\eta^2$ equal to zero, and excluding the derivatives $dn/d\eta$ and $d^2n/d\eta^2$, after simple transformations we will have the following:

$$\eta^2 = \frac{\left(n-\frac{1}{J\beta}\right)\left(n^2-n+\frac{1}{K\beta}\right)}{\left(n-1+\frac{1}{K\beta}\right)}, \tag{38}$$

$$(Jn\beta-1)\{2K^2(J+K)n[(n-1)\beta]^3 + K[3(J+K)n+J+3K] \times[(n-1)\beta]^2 + (J+6K)[(n-1)\beta]+2\} = 0. \tag{39}$$

These equations, together with initial Eqs. (34) and the condition for minimum of ω, determine the critical lines. The solution $n=1/(J\beta)$ of Eq. (39) corresponds to $\eta=0$, $\tilde{h}=0$, and

$$\tilde{E}_0 = \frac{1}{\beta}\left(\frac{K}{J} + \ln(\beta J - 1) + \ln 2\right). \tag{40}$$

It is just the critical line at $\tilde{h}=0$. If $J=0$, such a line does not exist at $\tilde{h}=0$. The critical line at $\tilde{h}\neq 0$ is determined by the root of the second factor of Eq. (39) that satisfies the condition for minimum of ω. This is a cubic with respect to $\beta(n-1)$ and it can be solved analytically, but in view of cumbersome analytical expressions for its roots we prefer to solve it numerically.

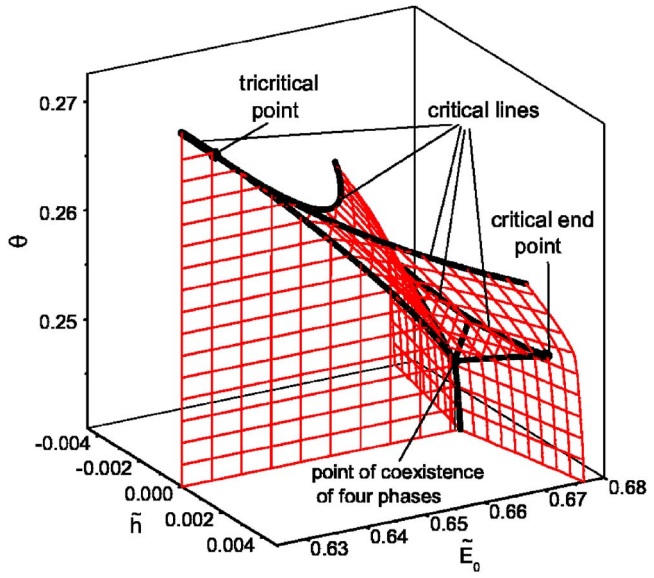

FIG. 4. (Color online) Phase diagram of the BEG model at $J=0.35$, $K=1.0$. All points of the phase coexistence surface, except the points of the critical line at $\tilde{h}=0$ (the thickest one), correspond to the first order phase transitions.

It is easy to find *the asymptotes of the critical lines*. It follows from Eq. (40) that

$$\lim_{\tilde{E}_0\to-\infty} \beta = \frac{1}{J}. \tag{41}$$

This is the asymptote of the critical line at $\tilde{h}=0$. The corresponding value of n tends to 1.

The asymptotes of the critical lines at $\tilde{h}\neq 0$ are as follows:

$$\tilde{E}_0 = |\tilde{h}| + \frac{J+K}{2}, \quad \beta = \frac{4}{J+K}. \tag{42}$$

The corresponding value of n tends to $\frac{1}{2}$.

C. Tricritical point, critical end point, and coexistence point of four phases

We can find the tricritical point, i.e., the point where the critical lines at $\tilde{h}=0$ and $\tilde{h}\neq 0$ meet, by substituting $n=1/(J\beta)$ (the root of the first factor) into the second factor of Eq. (39). Of three roots only one

$$\beta_{tc} = \frac{3J+2K}{(J+2K)J} \tag{43}$$

corresponds to the minimum for the thermodynamic potential. This solution defines the inverse tricritical temperature.

The tricritical point can be absent or the first order phase transition surface can be branched and thus, one of its critical point at $\tilde{h}=0$ will not be a tricritical one (Fig. 4). Then, in the

interval from this critical point until the critical end point (or to the coexistence point of four phases), η will be equal to zero and one obtains from Eqs. (34)

$$\frac{n}{1-n}e^{-\beta Kn} = 2e^{\beta\tilde{E}_0}. \tag{44}$$

Since the points from this interval corresponds to the first order phase transitions, Eq. (44) shall have two different roots that correspond to the same value of ω. It is evident that it is possible at the condition that the roots are equal to n and $1-n$ (at the critical point $n_1=n_2=\frac{1}{2}$), and, in addition, the following relation is obeyed

$$\tilde{E}_0 = \frac{K}{2} + \frac{1}{\beta}\ln 2. \tag{45}$$

In this way we have obtained the equation of the phase coexistence line starting at the critical point at $\tilde{h}=0$ ($\beta=4/K$) and ending at the coexistence point of four phases or at the critical end point.

The critical end point at $\tilde{h}=0$ shall satisfy both Eqs. (40) and (45). Hence, for the inverse temperature β_{ce} at the critical end point one has

$$e^{\beta_{ce}(K/2)} = e^{K/J}(\beta_{ce}J - 1). \tag{46}$$

Note, that the solution $\beta_{ce}=2/J$ of this equation is superfluous.

Let us find the limiting value of the ratio $R=J/K$ that bounds the region where the tricritical point exists. To do this we need to substitute the expression for inverse tricritical temperature in the previous equation. We will have

$$\exp\left(\frac{K(J-2K)}{2J(J+2K)}\right) = \frac{2J}{J+2K}, \tag{47}$$

from where

$$R_l = \frac{J}{K} \approx 0.263\,028\,3. \tag{48}$$

(The solution $J/K=2$ is superfluous.) If $R>R_l$ the tricritical point exists.

Let us also find the value of R that bounds above the region where the first order phase transition surface branches. Then the critical point with $\beta=4/K$, $\tilde{E}_0=(K/2)+(1/\beta)\ln 2=(K/2)+(K/4)\ln 2$, and $n=\frac{1}{2}$ moves down to the triple-point line and becomes thermodynamically unstable. Thus, the limiting value of R is determined by the following set of equations:

$$e^{8(J/K)\eta} = \frac{n-\eta}{n+\eta},$$

$$e^{8n-4} = \frac{n^2-\eta^2}{(1-n)^2},$$

$$\frac{1}{2}\frac{J}{K}\eta^2 + \frac{1}{2}n^2 + \frac{1}{4}\ln(1-n) = \frac{1}{8} - \frac{1}{4}\ln 2. \tag{49}$$

We have from it

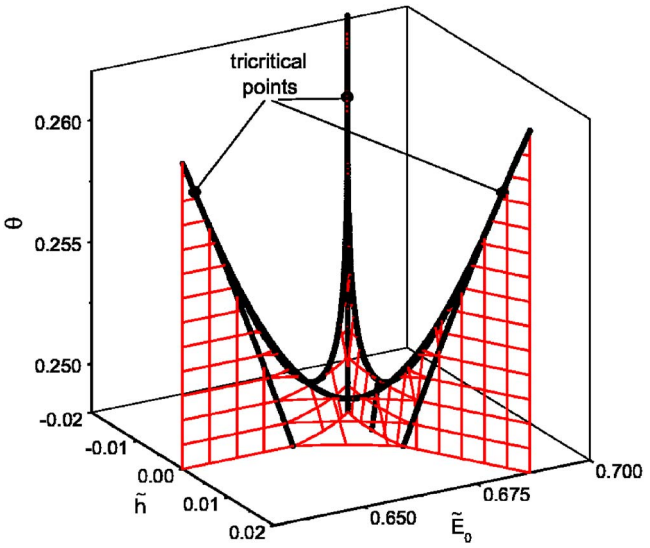

FIG. 5. (Color online) Phase diagram of the BEG model at the van Laar point ($J=1/3$, $K=1$). Tricritical temperature is the same for all three tricritical points.

$$R_u = \frac{J}{K} \approx 0.360\,402\,66. \tag{50}$$

If $R_l<R<R_u$ the first order phase transition surface is branched.

The set of Eqs. (49) represents a particular case of another set of equations, the nontrivial ($\eta\neq 0$) solution of which gives *the coexistence point of four phases*

$$e^{\beta K(1-2n)} = \frac{(1-n)^2}{n^2},$$

$$e^{\beta K(1-2n_1)} = \frac{(1-n_1)^2}{n_1^2-\eta^2},$$

$$e^{2\beta J\eta} = \frac{n_1-\eta}{n_1+\eta},$$

$$\frac{J}{2}\eta^2 + \frac{K}{2}n_1^2 + \frac{1}{\beta}\ln(1-n_1) = \frac{K}{2}n^2 + \frac{1}{\beta}\ln(1-n). \tag{51}$$

D. An analog of the van Laar point

Now, let us find an analog of the van Laar point,[20] i.e., the value of $R=J/K$, at which three tricritical points exist: one of them corresponds to the zero field and two others are symmetrical with respect to the $\tilde{h}=0$ plane (Fig. 5). The second factor of Eq. (39), being a cubic in $(n-1)\beta$, has therefore three real roots, two of them should be equal, i.e., its discriminant must be zero. This in turn produces another cubic in n with the coefficients that depend on R. It shall also have three real roots, two of which shall be equal, i.e., its discriminant must be zero. Hence, we obtain an equation in R

$$\Delta_n(\Delta_x\{2(R+1)nx^3+[3(R+1)n+R+3]x^2 + (R+6)x+2\})=0, \tag{52}$$

where $x=(n-1)\beta K$, and $\Delta_x[f(x)]$ denotes the discriminant of the equation $f(x)=0$ as an equation in x. Equation (52) has three real roots $(-1,0,\frac{1}{3})$ but only at

$$R=\tfrac{1}{3}, \tag{53}$$

three tricritical points exist and correspond to the same temperature

$$\beta_{tc}=\frac{27}{7K}. \tag{54}$$

At tricritical points the parameters have the following values:

$$n=\tfrac{11}{18}, \quad \eta=\pm\tfrac{1}{6},$$

$$\tilde{E}_0=\left(\tfrac{11}{18}+\tfrac{7}{54}\ln\tfrac{7}{4}\right)K\approx 0.683\,653K,$$

$$\tilde{h}=\pm\left(-\tfrac{1}{18}+\tfrac{7}{54}\ln\tfrac{7}{4}\right)K\approx\pm 0.0169\,87K. \tag{55}$$

The existence of three tricritical points with the same temperature at $R=\frac{1}{3}$ can be explained by the symmetry of the Hamiltonian (22) (see Sec. IV). This is an exact result though the tricritical temperature itself is calculated in the mean field approximation.

E. $J=0$ and $K=0$ cases

Let us consider now the particular cases: $J=0$ and $K=0$.

If $J=0$, one can obtain from Eqs. (34) and expression (35) for ω at $J=0$ the analytical expression for the phase coexistence surface [in the same manner as for Eq. (45)]

$$\tilde{E}_0=\frac{K}{2}+\frac{1}{\beta}\ln[2\cosh(\beta\tilde{h})]. \tag{56}$$

The corresponding phase diagram is shown in Fig. 6(a). The inverse critical temperature in this case is equal to

$$\beta=\frac{4}{K}. \tag{57}$$

The equation for n at the phase transition point writes

$$e^{-\beta K[n-(1/2)]}=\frac{1-n}{n}. \tag{58}$$

As we can see, n depends only on the temperature and the biquadratic interaction K. At the critical temperature $n=\frac{1}{2}$.

If $K=0$, we obtain the inverse temperature from Eq. (39)

$$\beta=-\frac{2}{J(1-n)}, \tag{59}$$

and the expression for the average dipole moment per site from Eq. (38)

$$\eta^2=\frac{3n-1}{2}. \tag{60}$$

These equations, together with Eqs. (34), define the critical line at $\tilde{h}\neq 0$, and the critical line at $\tilde{h}=0$ is defined in this case by the equation

$$e^{\beta\tilde{E}_0}=2(\beta J-1). \tag{61}$$

The inverse tricritical temperature is equal to

$$\beta_{tc}=\frac{3}{J}. \tag{62}$$

The phase diagram for the $K=0$ case is shown in Fig. 6(e).

VI. PHASE TRANSITIONS AND PHASE SEPARATIONS IN THE PSEUDOSPIN-ELECTRON MODEL WITH $S=1$ IN THE MEAN FIELD APPROXIMATION

Let us consider now the influence of electrons on the phase coexistence surface. As it was shown in Sec. I electrons cause the shift of the phase diagram. Since the shift depends on the temperature, the surface deforms [Figs. 6(b), 6(d), and 6(f)].

If the interaction of electrons with pseudospins does not depend on the orientation ($g=0$), then there is no shift along the axis h and the phase coexistence surface remains symmetric with respect to this axis. But there are shifts along the E_0 axis, which deform the surface. When the pseudospin-electron interaction ρ which does not depend on orientation is sufficiently strong, then the transitions from the phase with bigger n to the phase with smaller n, i.e., from the phase A or B in the phase C, can occur (Fig. 7) while the temperature increases. If there are no electrons, then such transitions may be impossible, for instance, when $J=0$ [see Fig. 6(a)].

In the case of fixed average number of electrons the phase separation takes place in a certain region of parameter values. As being already noted, it is crucial in the $J\neq 0$ case whether $\tilde{h}$ goes through zero or not when the electron chemical potential μ changes from $-\infty$ to $+\infty$ (the temperature and h being fixed). If not, then the separation region is bounded (Fig. 8), otherwise it is unbounded and extends to infinity along the $-E_0$ axis (Fig. 9). However, the separation caused by the fact that $\tilde{h}$ goes through zero produces the phases that differs by electron concentration only, because the concentration of intercalated particles does not change on the $\tilde{h}=0$ surface.

The phase separation region in the (n,θ) plane for the BEG model at $\tilde{h}=0$ is shown in Fig. 10. This diagram is typical for symmetrical binary mixture (see for example Ref. 21 and also Ref. 18. The influence of the pseudospin-electron interaction on the diagram is shown in Fig. 11. The interaction with electrons smoothes out the separation curve; the λ-line disappears.

Let us study the behavior of the average number of electrons per site n in relation to the chemical potential of intercalated particles $-E_0$ when the temperature θ and the average number of electrons per site n_e are fixed (in the real interca-

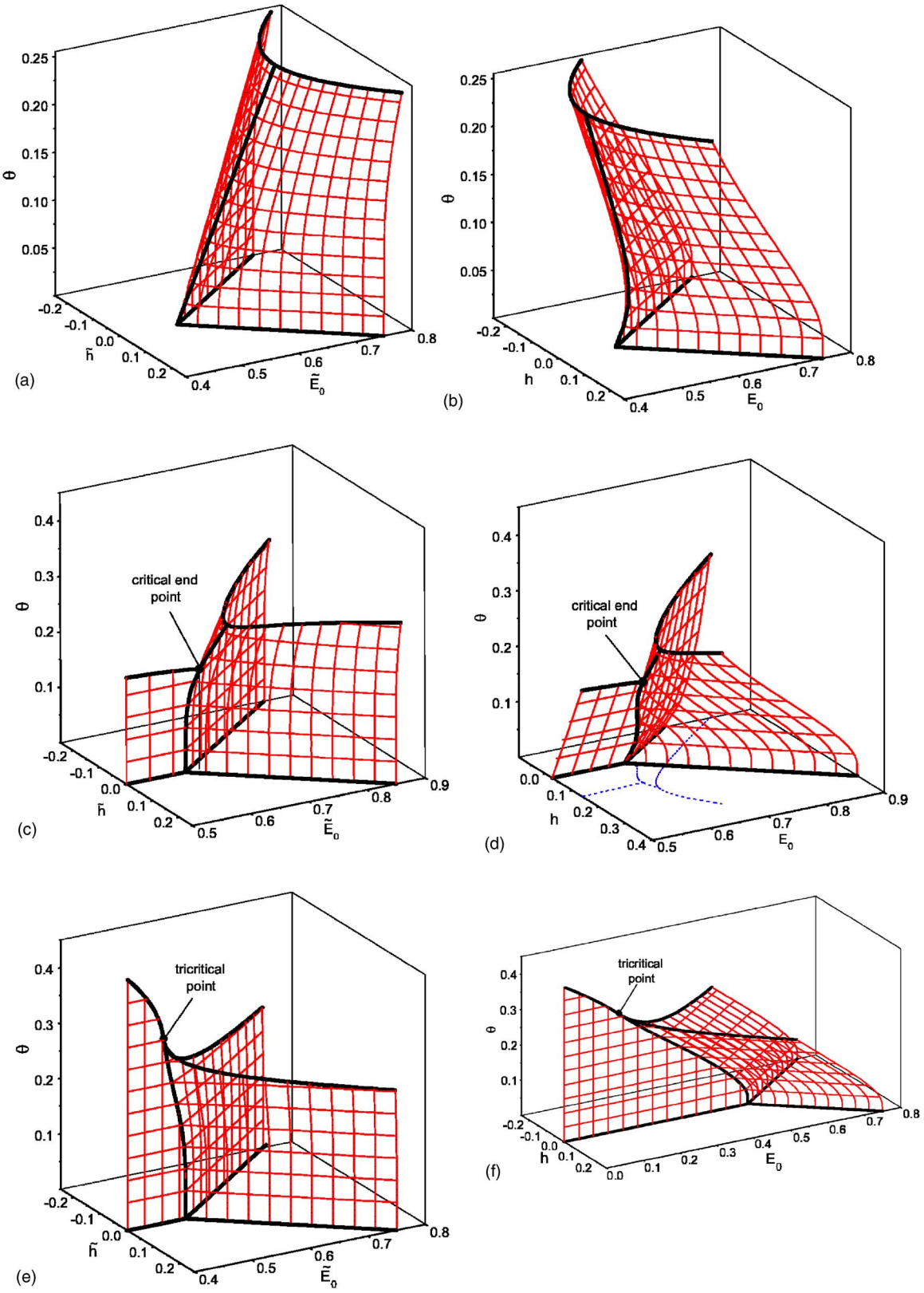

FIG. 6. (Color online) (a), (c), (e) Phase diagrams of the BEG model at: (a) $J=0$, $K=1.0$; (c) $J=0.2$, $K=1.0$; (e) $K=0$, $J=1.0$. (b), (d), (f) Phase diagrams of the $S=1$ pseudospin-electron model at: (b) $J=0$, $K=1.0$, $g=0$, $\rho=1.0$, $U=0.2$, $\mu=-0.1$; (d) $J=0.2$, $K=1.0$, $g=1.15$, $\rho=1.0$, $U=0.2$, $\mu=-0.1$; (f) $J=1.0$, $K=0$, $g=0$, $\rho=1.0$, $U=0.2$, $\mu=-0.1$. In (d) projections of the thick lines on (h,E_0) plane are indicated. All points of the phase coexistence surfaces, except the points of critical lines at $\tilde{h}=0$ or $h=0$ [(c), (e), and (f)], correspond to the first order phase transitions.

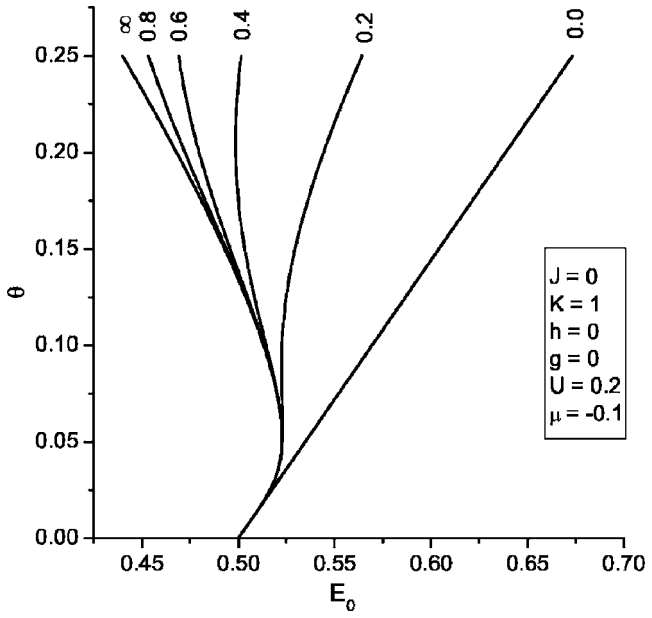

FIG. 7. Phase diagrams of the $S=1$ pseudospin-electron model at $J=0$, $h=0$ and different values of ρ. Phase transitions from the phase with bigger n to the phase with smaller n or even reentrance phase transitions are possible while the temperature increases (they are impossible at $\rho=0$).

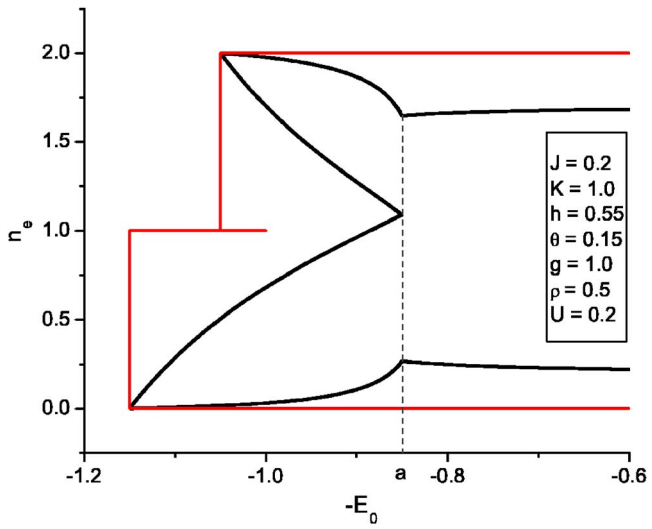

FIG. 9. (Color online) Phase separation at zero (straight lines) and nonzero temperature and $J\neq 0$. If n_e and E_0 are such that the point $(-E_0, n_e)$ drops into separation region, the separation into two phases with different values of n_e occurs at the same value of E_0. If $-E_0 < a$ the phases differ also by n; if $-E_0 > a$ the phases differ only by n_e, n being the same $(J\neq 0)$.

lation process n_e does not change). To do that one has to add the equation for the chemical potential (13) to Eqs. (34) and (35). If $\mu=\infty$, then $n=0$. When $-E_0$ increases, then n increases monotonically as long as the point $(-E_0, n_e)$ is outside of the separation region. In this region two phases with different average numbers n_1 and n_2 of particles per site exist. As far as we are considering the $J=0$ case the number n_1 and n_2 do not depend on $-E_0$, they depend on the temperature and K only [see Eq. (58)]. Outside the separation region, n monotonically increases again, tending asymptotically to 1. Figure 12 shows how the behavior of $n(-E_0)$ depends on ρ and the temperature. h is chosen near to zero.

As illustrated in Fig. 12, with the increase of ρ the separation region moves in the direction of larger values of the chemical potential of intercalated particles. The separation region can narrow first and expand afterwards, in relation to g. The increase of g narrows the separation region and, of course, it narrows with the increase of the temperature and disappears completely at the critical temperature. Furthermore, the difference n_1-n_2 of particle concentrations of two phases decreases with the temperature increase. The value of n_e also influences significantly the width of the phase separation region.

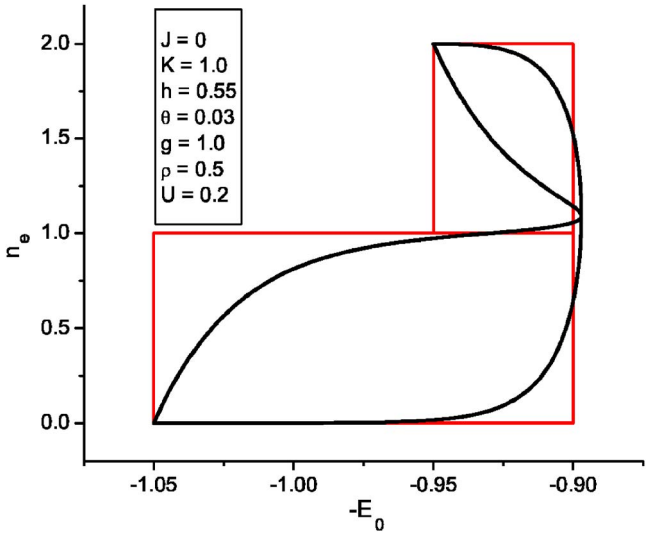

FIG. 8. (Color online) Phase separation at zero (straight lines) and nonzero temperature and $J=0$.

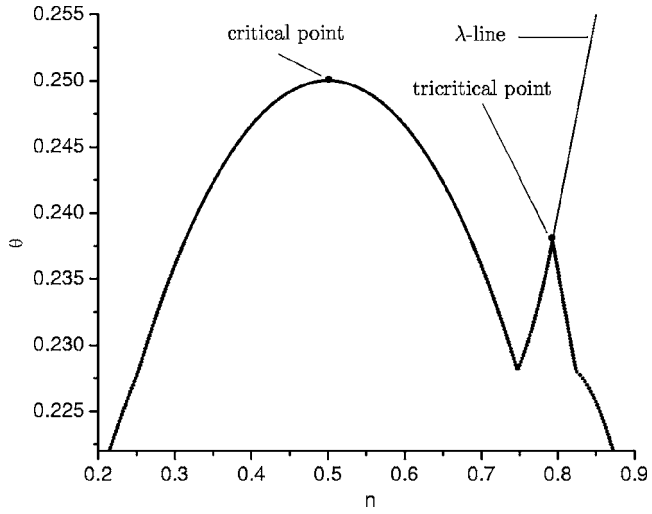

FIG. 10. Phase separation in the (n, θ) space for the BEG model. $J=0.3$, $K=1$, $\tilde{h}=0$.

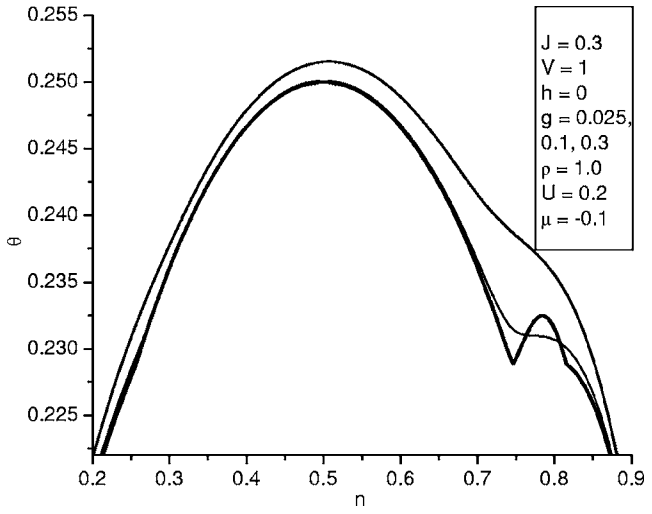

FIG. 11. Phase separation curves in the (n,θ) space for the pseudospin-electron model at different values of the pseudospin-electron interaction g. The intercalation with electrons smoothes out the separation curve.

VII. CONCLUSIONS

A pseudospin-electron model based on the BEG model is proposed and has been found to be applicable to describe the essential features of the intercalation in layered crystals. Due to the one-site nature of the electron-electron and pseudospin-electron interactions in the model, the influence of the electron subsystem can be taken into account exactly by reducing the partition function of the system to the partition functions of independent pseudospin and electron subsystems. The fields of the effective pseudospin subsystem turned to be shifted and depend on the temperature and the parameters related to the electrons. In the case of nearest neighbor interactions it is possible to construct the exact ground-state phase diagram for the pure pseudospin model. It allows one to study phase transitions and phase separations in the pseudospin-electron model exactly at zero temperature.

At any fixed temperature the influence of electrons leads to the shifts of the phase coexistence lines along the h and E_0 axes. The shifts depends on the temperature, therefore the phase coexistence surface deforms, and if the pseudospin-electron interaction which depends on the orientation of pseudospins is nonzero ($g \neq 0$), then the phase diagram is no longer symmetric with respect to the field h.

In the case of fixed average number of electrons n_e or intercalated particles $n=\langle S_i^{\tau 2}\rangle$ per site the phase separation takes place. We studied the phase separation when n_e is fixed. Several types of the phase separation regions are then possible at zero temperature in the $(-E_0,n_e)$ plane. Their width depends on the field strength h. If the interaction between pseudospins does not depend on their mutual orientation (the $J=0$ case), then the separation region is bounded, otherwise the phase separation regions unbounded on one side are possible.

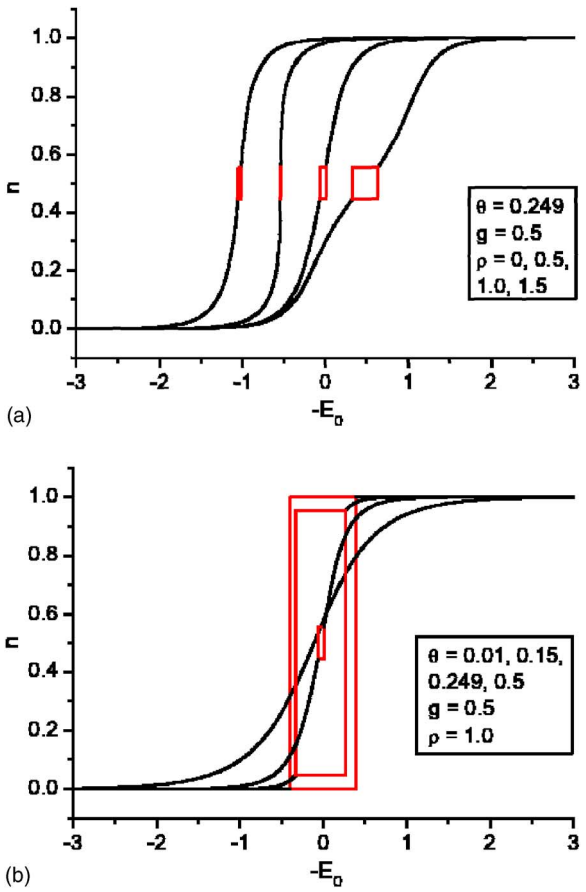

FIG. 12. (Color online) Dependence of the average number n of intercalated particles per site on their chemical potential $-E_0$. $J=0$, $K=1$, $h=0.001$, $n_e=1$, $U=0.2$. The rectangles indicate the separation region. The temperature $\theta=0.249$ is very close to the critical one ($\theta_{cr}=0.25$).

The application of the pseudospin-electron model to the intercalation process in layered crystals which is the subject of this study leads to an important conclusion: the phase separation into the phases with different concentrations of particles is caused by the fact that *the number of electrons* that interact with intercalated particles is fixed, even if the number of latter ones is not fixed. Thus, the insular structure of intercalated layers observed in the experiments over a certain range of chemical potential of intercalated particles is due to their interaction with the electrons of basic layers. If the number of intercalated particles is also fixed, then a "double" phase separation occurs. We will consider this case in our future study.

ACKNOWLEDGMENT

We thank Dr. Ya. Ilnytskyi for his careful reading of the manuscript.

[1] L. Schlapbach and A. Zuttel, Nature (London) **414**, 353 (2001).
[2] W. R. Mckinnon and R. R. Haering, in *Modern Aspect of Electrochemistry* No. 15, edited by R. E. White, J. O'M. Bockris, and B. E. Conway (Plenum, New York, 1983).
[3] *Handbook of Batteries* (3rd ed.), edited by D. Linden and T. B. Reddy (McGraw-Hill, New York, 2001).
[4] C. G. Granqvist, *Handbook of Inorganic Electrochromic Materials* (Elsevier, New York, 1995).
[5] J. S. Slusky *et al.*, Nature (London) **410**, 343 (2001).
[6] W. Y. Liang, in *Intercalation in Layered Materials*: *Proceedings of the 10th Course of the Erice Summer School* (Plenum Press, New York, 1986), pp. 31–74.
[7] E. Sandre, R. Brec, and J. Rouxel, J. Solid State Chem. **88**, 267 (1990).
[8] Z.-X. Cai and S. D. Mahanti, Phys. Rev. B **36**, 6928 (1987).
[9] I. V. Stasyuk, in *High-Lights In Condensed Matter Physics*, AIP Conf. Proc., No. 695 (Melville, New York, 2003), pp. 281–290.
[10] Yu. I. Dublenych, Report No. ICMP-01-01U, 2001 (unpublished) (in Ukrainian).
[11] I. V. Stasyuk, A. M. Shvaika, and O. D. Danyliv, Mol. Phys. Rep. **9**, 61 (1995).
[12] E. V. Vakarin, J. P. Badiali, M. D. Levi, and D. Aurbach, Phys. Rev. B **63**, 014304 (2001).
[13] M. Blume, V. J. Emery, and R. B. Griffiths, Phys. Rev. A **4**, 1071 (1971).
[14] D. Mukamel and M. Blume, Phys. Rev. A **10**, 610 (1974).
[15] J. Sivardière and J. Lajzerowicz, Phys. Rev. A **11**, 2079 (1975).
[16] J. Sivardière, in *Critical and Multicritical Points in Fluids and Magnets*, edited by A. Pekalsky Lecture Notes in Physics Vol. 206 (Springer, Berlin, 1984), pp. 247–289.
[17] W. Hoston and A. N. Berker, Phys. Rev. Lett. **67**, 1027 (1991).
[18] I. V. Stasyuk, K. D. Tovstyuk, O. B. Gera, and O. V. Velychko, Report No. ICMP-02-09U, 2002 (unpublished) (in Ukrainian).
[19] Yu. I. Dublenych, Phys. Rev. B **71**, 012411 (2005).
[20] P. H. E. Meijer, M. Keskin, and I. J. Pegg, J. Chem. Phys. **88**, 1976 (1988).
[21] N. B. Wilding, F. Schmid, and P. Nielaba, Phys. Rev. E **58**, 2201 (1998).